The American Journal of Pathology, Vol. 171, No. 4, October 2007

DOI: 10.2353/ajpath.2007.070190

Vascular Biology, Atherosclerosis and Endothelium Biology

Disordered Purinergic Signaling Inhibits Pathological Angiogenesis in *Cd39/Entpd1*-Null Mice

Shaun W. Jackson,* Tomokazu Hoshi,† Yan Wu,* Xiaofeng Sun,* Keiichi Enjyoji,* Eva Cszimadia,* Christian Sundberg,‡ and Simon C. Robson*

From the Department of Medicine, Beth Israel Deaconess Medical Center, Harvard Medical School, Boston, Massachusetts; the Second Department of Surgery,† Asahikawa Medical College, Asahikawa, Hokkaido, Japan; and the Department of Medical Biochemistry and Microbiology,‡ Biomedical Center and Children's Academic Hospital, Uppsala, Sweden*

CD39/ecto-nucleoside triphosphate diphosphohydrolase-type-1 (ENTPD1) is the dominant vascular ecto-nucleotidase that catalyzes the phosphohydrolysis of extracellular nucleotides in the blood and extracellular space. This ecto-enzymatic process modulates endothelial cell, leukocyte, and platelet purinergic receptor-mediated responses to extracellular nucleotides in the setting of thrombosis and vascular inflammation. We show here that deletion of *Cd39/Entpd1* results in abrogation of angiogenesis, causing decreased growth of implanted tumors and inhibiting development of pulmonary metastases. Qualitative abnormalities of *Cd39*-null endothelial cell adhesion and integrin dysfunction were demonstrated *in vitro*. These changes were associated with decreased activation of focal adhesion kinase and extracellular signaling-regulated kinase-1 and -2 in endothelial cells. Our data indicate novel links between CD39/ENTPD1, extracellular nucleotide-mediated signaling, and vascular endothelial cell integrin function that impact on angiogenesis and tumor growth. *(Am J Pathol 2007, 171:1395–1404; DOI: 10.2353/ajpath.2007.070190)*

CD39/ecto-nucleoside triphosphate diphosphohydrolase-1 (ENTPD1) catalyzes phosphohydrolysis of extracellular nucleoside di- and triphosphates to the monophosphate derivatives.[1] Extracellular nucleotides released by platelets, leukocytes, and vascular cells signal endothelial cells through type-2 purinergic (P2) receptors termed P2Y (G protein-coupled receptors) or P2X (ligand-gated channels).[2] Deletion of *Cd39* has been shown to perturb P2 receptor signaling in *Cd39*-null mice, resulting in platelet dysfunction and disordered thromboregulation.[3] Activation of P2 receptors appears to influence endothelial cell chemotactic and mitogenic responses *in vitro*.[4] These data suggest roles for CD39 in modulating such responses during angiogenesis, and Matrigel plug-induced vascularization can be shown to be absent in *Cd39*-null mice.[5]

Angiogenesis is important in cancer progression and crucial for tumor growth and metastasis.[6,7] The process of neovascularization is influenced by integrins,[8] including endothelial $\alpha_V\beta_3$.[9] $P2Y_2$ co-localizes with $\alpha_V\beta_3$ to modulate endothelial integrin function and migration.[10] Ligand binding to integrins induces phosphorylation of focal adhesion kinase (FAK), activating extracellular signaling-regulated kinase-1 and -2 (ERK1/2).[11,12] Activation of mitogen-activated protein kinase ERK1/2 promotes angiogenesis by blocking apoptosis and promoting proliferation.[12]

These observations suggest potential functional links between CD39, P2Y receptors, and endothelial integrins. We have therefore investigated the effects of *Cd39* deletion on tumor angiogenesis and metastasis *in vivo* and studied underlying pathogenic mechanisms *in vitro*.

Materials and Methods

Antibodies and Other Reagents

Antibodies against PECAM, pan-endothelial antigen (MECA-32), CD3ε, CD19, CD41, LY-6G, and LY-6C were from BD Biosciences (San Jose, CA). Antibodies against perlecan and pericyte marker (NG2) were from Chemicon (Temecula, CA). Antibodies against platelet-derived growth factor-β, FLK-1, and α_V-integrin were from Santa Cruz Biotechnology (Santa Cruz, CA). Antibodies to the macro-

Supported by the National Institutes of Health (grants HL63972, AI45897, and HL076540).

C.S. and S.C.R. are joint senior authors.

Accepted for publication June 27, 2007.

Current address of S.W.J.: Children's Hospital Boston, Harvard Medical School, Boston, MA.

Address reprint requests to Simon C. Robson, Department of Medicine, Beth Israel Deaconess Medical Center, Harvard Medical School, Boston, MA 02215. E-mail: srobson@bidmc.harvard.edu.

phage marker (F4/80) were from Serotec (Raleigh, NC). Antibodies against Fab2 and fibrinogen/fibrin were from DAKO (Carpinteria, CA). Antibodies against reticular fibroblasts (clone ER-TR7) were from Cedarlane Laboratories (Burlington, ON, Canada). The fluorescein-labeled anti-smooth muscle α-actin and MMP-9 antibodies were from Sigma-Aldrich (St. Louis, MO). Antibodies against FAK and phosphorylated-FAK (Tyr397) were purchased from BD Transduction Laboratories (Franklin Lakes, NJ). Antibodies against ERK1/2 and phosphorylated ERK 1/2 (Thr202/Tyr204) were from Cell Signaling Technology (Beverly, MA). Secondary antibodies were from Vector Laboratories (Burlingame, CA). The luciferase assay kit was from Promega (Madison, WI). Grade VII potato apyrase (a soluble NTPDase) and vitronectin from rat plasma were from Sigma-Aldrich.

Mouse Tumor Inoculation

Animals were housed in accordance with the guidelines from the American Association for Laboratory Animal Care. The Beth Israel Deaconess Medical Center Institutional animal care and use committees approved all research protocols. C57BL/6X129svj or C57BL6 backcrossed (for more than six generations) strains of wild-type and type-matched *Cd39*-null mice were inoculated with 3.0×10^6 cells B16-F10 melanoma ($n = 8$ and 6), B16-CG (stable β-HCG expression vector transfected) melanoma[13] ($n = 4$), or Lewis lung cancer (LLC) cells ($n = 4$) into the dorsal subcutaneous space. Tumor size was measured daily, and the tumor volume was calculated using the formula $V = \pi L.W^2/6$, where L is the longer diameter and W the short diameter of tumor. Wild-type and *Cd39*-null mice were also injected with 5.0×10^5 B16-F10 melanoma into the subperitoneal plane of an abdominal wall flap ($n = 6$). The subperitoneal tumors were examined at 2-day intervals by limited laparotomy, the tumor size measured, and new blood vessels growing into the tumor were counted by microscopy. At 15 days, mice were sacrificed and the tumors analyzed by immunohistochemistry.

Measurement of Mouse β-HCG Excretion

The urine of mice inoculated with B16-CG melanoma cells was collected as described.[13] Urine β-HCG was measured with β-HCG enzyme-linked immunosorbent assay kits (Alpha Diagnostic, San Antonio, TX) and urine creatinine with the Creatinine assay kit (Sigma Diagnostics, Inc., St. Louis, MO).

Pulmonary Metastasis Model

B16-F10 cells (1.5×10^5) were injected into the inferior vena cava of C57BL/6X129svj strain wild-type ($n = 6$) and type-matched *Cd39*-null mice ($n = 4$). After 15 days, the mice were euthanized and the pulmonary metastases analyzed for size and number.

Measurement of Tumor Cell Sequestration in the Pulmonary Vasculature

Luciferase-expressing B16/F10 cells (lucB16/F10) were established as described.[14] luc-B16/F10 cells (5×10^5) were injected into penile veins of age- and sex-matched C57/BL6 wild-type ($n = 3$) and *Cd39*-null mice ($n = 3$). One hour later, the mice were sacrificed, the lungs snap-frozen in liquid nitrogen, and the tissue homogenized in luciferase lysis buffer (Promega). The 20 μl of lung homogenate was added to 100 μl of luciferase assay buffer (Promega) and luciferase activity was measured using a luminometer. Luciferase activity was expressed as relative light units (RLUs) normalized for protein content and background of control lungs.

Immunohistochemical Staining

Frozen sections of implanted B16-F10 tumors were analyzed by immunohistochemistry and immunofluorescence as described.[5]

Primary Lung Endothelial Cell Isolation

Wild-type and *Cd39*-null mouse lungs were minced, collagenase-digested (Life Technologies, Inc., Grand Island, NY), and strained and the resulting cell suspension plated on flasks coated with 0.2% gelatin (Sigma). Endothelial cells were purified by a single negative (FCγ-RII/III antibody; Pharmingen, La Jolla, CA) and two positive (ICAM-2; Pharmingen) sorts using anti-rat IgG-conjugated magnetic beads (Dynal; Invitrogen, Carlsbad, CA) producing a >98% pure population.

Endothelial Cell Proliferation and Growth Factor Signaling

Wild-type and *Cd39*-null C57BL6 endothelial cells were treated for 24 hours with vascular endothelial growth factor (VEGF) (10 ng/ml), insulin (10 nmol/L), hepatocyte growth factor (50 ng/ml), fibroblast growth factor (10 ng/ml), or insulin-like growth factor-1 (10 ng/ml). Cells were then pulsed with [^{3}H]thymidine for 8 hours and uptake measured as described.[15] VEGF-induced activation of ERK1/2 was measured after stimulation of wild-type and *Cd39*-null endothelial cells with VEGF (10 ng/ml) for 5 minutes. ERK1/2 activation was expressed as the ratio of phosphorylated to unphosphorylated ERK1/2 after Western blot analysis.

Adhesion Assays

Adhesion assays were performed as previously described.[16] For the pretreatment experiments to deplete extracellular nucleotides, cells were preincubated with a soluble NTPDase, grade VII apyrase (5 U/ml), in serum-free conditions for 6 hours before assay. For

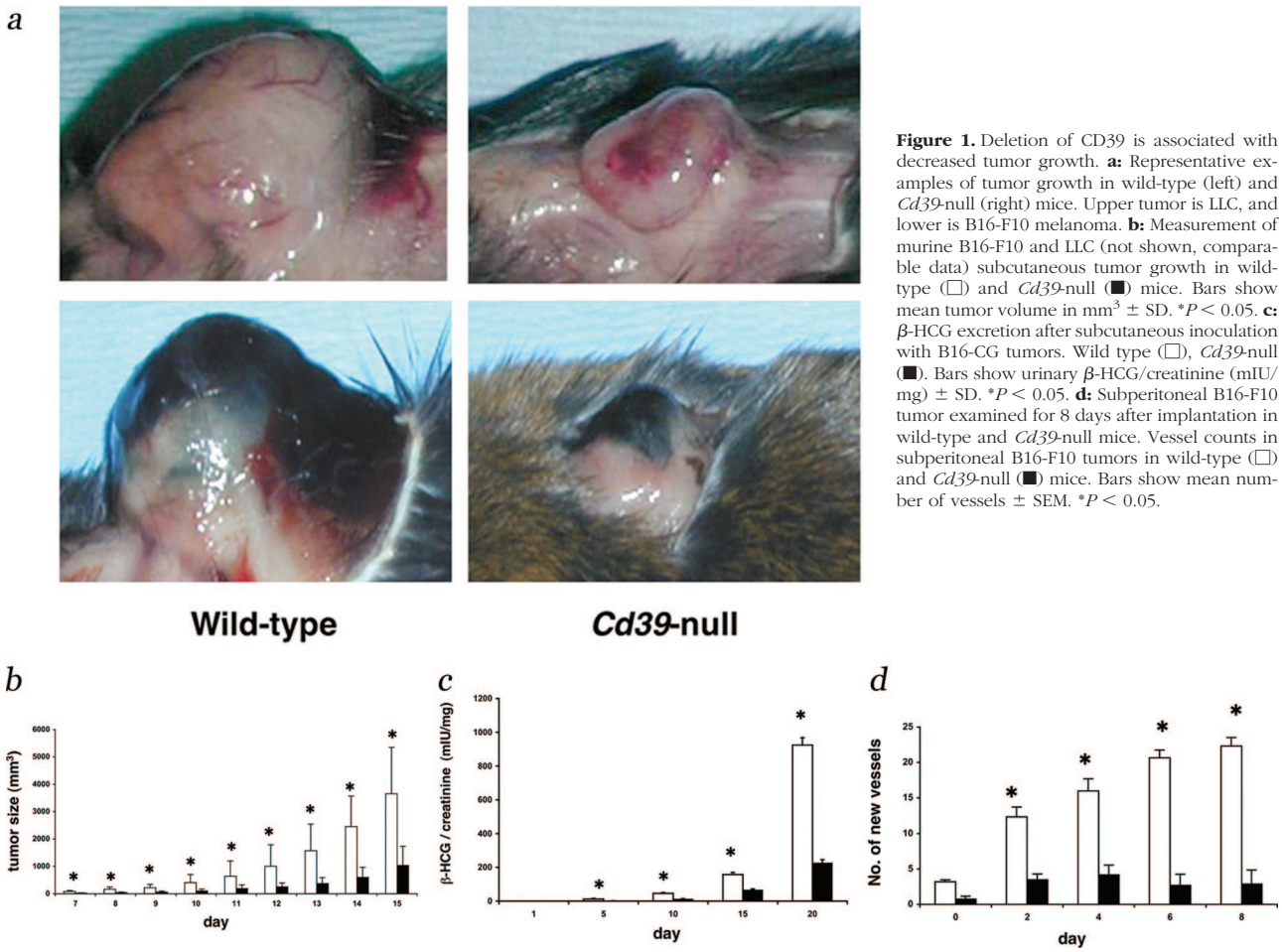

Figure 1. Deletion of CD39 is associated with decreased tumor growth. **a:** Representative examples of tumor growth in wild-type (left) and *Cd39*-null (right) mice. Upper tumor is LLC, and lower is B16-F10 melanoma. **b:** Measurement of murine B16-F10 and LLC (not shown, comparable data) subcutaneous tumor growth in wild-type (□) and *Cd39*-null (■) mice. Bars show mean tumor volume in mm^3 ± SD. $^*P < 0.05$. **c:** β-HCG excretion after subcutaneous inoculation with B16-CG tumors. Wild type (□), *Cd39*-null (■). Bars show urinary β-HCG/creatinine (mIU/mg) ± SD. $^*P < 0.05$. **d:** Subperitoneal B16-F10 tumor examined for 8 days after implantation in wild-type and *Cd39*-null mice. Vessel counts in subperitoneal B16-F10 tumors in wild-type (□) and *Cd39*-null (■) mice. Bars show mean number of vessels ± SEM. $^*P < 0.05$.

integrin activation experiments, manganese chloride ($MnCl_2$, 500 μmol/L) was added to cells during the adhesion process.

α_V Integrin Expression

Wild-type and *Cd39*-null endothelial cells were stimulated with 100 μmol/L UTP for 0, 2, 4, or 6 hours. Cells were lysed in radioimmunoprecipitation assay buffer, and 250 μg of protein immunoprecipitated using α_V integrin antibody. Total α_V expression was determined in a semiquantitative manner by Western blot.

FAK and ERK1/2 Activation Assay

Wild-type and *Cd39*-null endothelial cells were serum-starved for 30 hours, trypsinized, and added to vitronectin-precoated dishes. Total cell extracts were prepared, and sodium dodecyl sulfate-polyacrylamide gel electrophoresis and Western blotting with antibodies to FAK, phosphorylated FAK (Tyr397), ERK1/2, and phosphorylated ERK1/2 (Thr202/Tyr204) were performed. For apyrase pretreatments, cells were incubated with grade VII apyrase (5 U/ml) for 6 hours, trypsinized, washed, and plated onto vitronectin.

Statistical Analysis

The Student's *t*-test with one-tailed distribution was used to analyze data (Excel; Microsoft, Redmond, WA).

Results

Transplanted Tumor Growth Is Decreased in Cd39-Null Mice

Matched wild-type and *Cd39*-null mice were injected subcutaneously with murine melanoma (B16-F10, American Type Culture Collection: CRL-6457; Manassas, VA) or lung carcinoma (LLC, American Type Culture Collection: CRL-1642) cells. The growth of both tumors was significantly attenuated in *Cd39*-null mice (Figure 1a). Wild-type mice had significantly larger B16-F10 (Figure 1b) and LLC (not shown) tumor volumes at 1 week. Tumor growth then entered the exponential phase in wild-type mice but in *Cd39*-null mice was severely retarded up to 15 days (Figure 1, a and b). Release of β-HCG after implantation of B16-CG melanoma cells was also used to estimate tumor volume.[13] β-HCG excretion correlates well with tumor volume in this model ($R^2 = 0.96$, data not shown). Urine β-HCG excretion was significantly decreased in *Cd39*-null mice (Figure 1c).

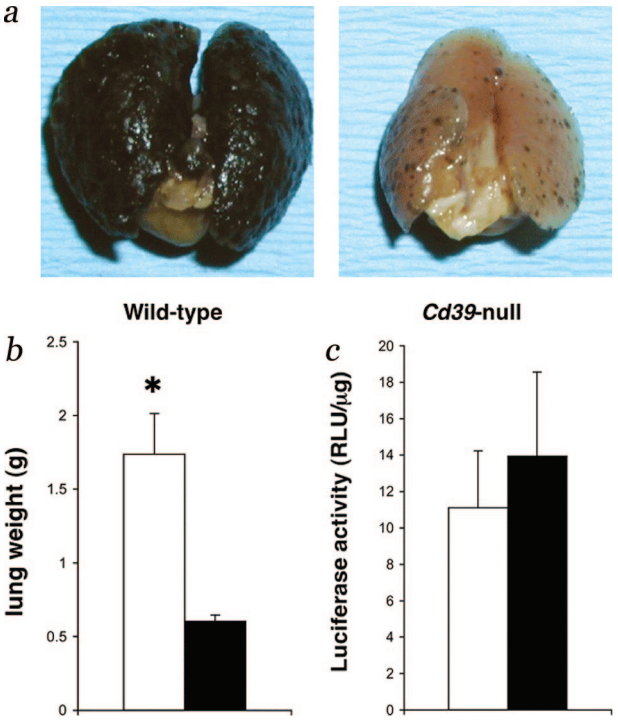

Figure 2. Decreased growth of inoculated tumor metastases, in *Cd39*-null mice. **a:** Representative examples of wild-type (right) and *Cd39*-null (left) mouse lungs at 15 days after tumor cell injection intravenously. **b:** Wild-type (□) and *Cd39*-null (■) lung weights 15 days after intravenous tumor injection. **a** and **b:** Mice were injected with 1.5×10^5 B16-F10 cells per 25 g of body weight into the inferior vena cava and lungs were examined at 15 days. Bars represent mean weight ± SEM. $^*P < 0.006$. **c:** Retention of cell-associated luciferase activity in wild-type (□) and *Cd39*-null (■) mice 1 hour after injection of 5×10^5 luciferase-expressing B16-F10 cells (lucB16/F10). Bars represent relative light units (RLUs) per μg of lung ± SD.

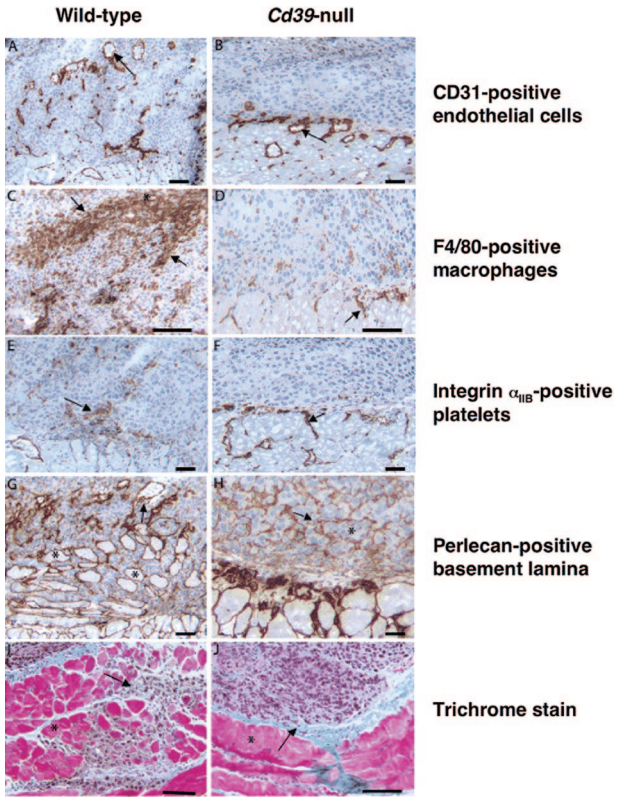

Figure 3. Immunohistochemistry of B16-F10 tumors. Tumors were implanted and grown in the subcutaneous space in wild-type (**A**, **C**, **E**, **G**, and **I**) and *Cd39*-null (**B**, **D**, **F**, **H**, and **J**) mice. **A** and **B:** CD31-positive endothelial cells can be seen infiltrating tumor (**arrow**) in wild-type (**A**), but not *Cd39*-null animals (**B**). Endothelial cells are confined to the interface between tumor and surrounding tissue in *Cd39*-null mice (**arrow**). **C** and **D:** There was marked infiltration of F4/80-positive macrophages (**arrows**) in tumors grown in wild-type animals (**C**), in particular in the necrotic central zone (*). In contrast, macrophages were mostly absent within tumors grown in *Cd39*-null mice (**D**). **E** and **F:** Platelets (integrin α_{IIb}-positive) were associated with vessels within the tumor mass in wild-type mice (**E**) but were confined to the tumor interface in *Cd39*-null animals (**F**). **G** and **H:** In tumors grown in wild-type mice (**G**), perlecan staining showed basal lamina associated with tumor vessels (**arrow**) but not tumor cell nests. In contrast, in tumors grown in *Cd39*-null mice (**H**), which were primarily devoid of vasculature, basal lamina divided individual tumor cell nests into gland-like structures (*). **I** and **J:** Trichrome staining showed tumors cells (**arrow**) in wild-type mice (**I**) invading deep into the underlying muscle layer (*). In contrast, in tumors grown in *Cd39*-null mice (**J**), tumor cell invasion was absent, and the tumor mass and muscle layer (*) was clearly separated. Scale bars = 20 μm.

Tumor Angiogenesis Is Decreased in Cd39-Null Mice

Direct visualization of B16-F10 tumors in wild-type and *Cd39*-null mice 7 days after implantation confirmed poor tumor growth in *Cd39*-null mice (not shown). In addition, this model allowed direct assessments of neovascularization of the tumor by dissection microscopy. By 2 days after tumor injection, wild-type mice had evidence of new vessels infiltrating the tumor that increased steadily in number (Figure 1d). This neovascularization was abrogated in *Cd39*-null mice.

Tumor Metastases Are Decreased in Cd39-Null Mice

We next studied development of pulmonary metastases in wild-type and *Cd39*-null mice after intravascular inoculation of 1.5×10^5 B16-F10, as described.[17] Wild-type lungs became infiltrated with tumor cells and, at 15 days after intravascular injection, tumor metastases had increased in size and replaced the entire lung (Figure 2a). In contrast, *Cd39*-null lungs had limited tumor numbers that were also of smaller size. Wild-type lung weights were also significantly increased more than *Cd39*-null levels (1738-mg wild type versus 604-mg *Cd39*-null, $P < 0.01$; Figure 2b).

We next examined sequestration of tumor cells within the lung vasculature by determining short-term retention of injected tumor cells expressing luciferase. These experiments were done in wild-type and *Cd39*-null mice and assays conducted at 1 hour after injection of 5×10^5 luciferase-expressing B16/F10 cells (lucB16/F10). There was no significant difference in luciferase activity in wild-type and *Cd39*-null lungs (wild-type 11.1 ± 3.1 RLU/μg versus *Cd39*-null 13.9 ± 4.6 RLU/μg, $P = 0.1$). The decreased development of lung metastases in *Cd39*-null mice did not appear secondary to decreased seeding of circulating tumor cells within the pulmonary vasculature (Figure 2c). These data suggest that the decreased development of pulmonary metastases in *Cd39*-null animals

might be secondary to subsequent failure of growth and potentially defective angiogenesis with an endothelial cell defect.

Immunopathology

Staining with the endothelial marker PECAM-1 showed growth of blood vessels into the implanted B16-F10 tumor mass in wild-type mice (Figure 3A). In contrast, tumors in *Cd39*-null mice were devoid of vessels, which were confined to the interface between the tumor and adjacent normal tissue (Figure 3B).

Significant numbers of macrophages had migrated to the interface between tumor tissue and adjacent normal tissue and into the viable and necrotic areas within the tumors in wild-type animals (Figure 3C). In contrast, few macrophages were noted in *Cd39*-null sections (Figure 3D). Tumors and surrounding tissues in wild-type and *Cd39*-null animals contained similar amounts of B and T lymphocytes as well as granulocytes (Table 1). Platelet deposition was noted within vessels in the tumors in wild-type mice (Figure 3E) but was confined to the tumor interface in *Cd39*-null animals (Figure 3F).

Basal lamina deposition, namely anti-perlecan staining, was noted around tumor vessels and muscle bundles in wild-type mice (Figure 3G). In *Cd39*-null mice, this was present in adjacent normal vessels encompassing tumor mass (Figure 3H). Tumor cell islands were enveloped in basal lamina, forming glandular-like structures in *Cd39*-null mice (Figure 3H). This was absent in tumors in wild-type mice (Figure 3G) potentially indicating a higher level of tumor cell differentiation in tumors in *Cd39*-null mice. In addition to enhanced growth, tumors in wild-type mice were further capable of invading the underlying dermal muscle fascia (Figure 3I), whereas those in *Cd39*-null mice did not display invasive behavior (Figure 3J).

In tumors implanted into wild-type mice, vessels were partially enveloped by pericytes and surrounded by interstitial fibroblasts (Figure 4D). In contrast, tumors in *Cd39*-null mice were devoid of endothelial cells, pericytes, and fibroblasts (Figure 4H), indicating pluripotent cellular migration defects in *Cd39*-null mice. Markers of blood vessel activation (namely dissolution of the enveloping basal lamina, increased pericyte expression of NG2, platelet-derived growth factor-β receptors, decreased pericyte expression of smooth muscle α-actin, and increased endothelial expression of VEGFR2 receptors) were apparent at the interface between tumor and normal adjacent tissue in wild-type mice. These changes were not seen in *Cd39*-null mice (Table 1). Platelet and fibrin deposition were noted in and around infiltrating vessels in wild-type tumors (Figure 4L) but in *Cd39*-null mice were confined to the rim of tissue surrounding the tumor (Figure 4P). Thus, despite deposition of a provisional matrix, blood vessels failed to appropriately activate and migrate into the tumor mass in *Cd39*-null mice (Table 1).

Table 1. Distribution of Cell-Type-Specific Markers, Cellular Activation Markers, and Extracellular Matrix Components in Wild-Type and *Cd39*-Null Mice after B16-F10 Tumor Implantation

	Normal dermis	Tumor interface	Tumor tissue
Endothelium			
PECAM-1			
Wild type	++	++	++
Cd39-null	++	++	−
Panendothelial marker			
Wild type	++	++	++
Cd39-null	++	++	−
VEGFR2 receptor			
Wild type	+	++	++
Cd39-null	+	++	−
Pericytes/myofibroblasts			
α-SMA			
Wild type	++	+	++
Cd39-null	++	++	−
PDGF-β receptors			
Wild type	+	++	++
Cd39-null	+	+	−
NG2			
Wild type	+	++	++
Cd39-null	+	+	−
Reticular fibroblasts			
Wild type	+	++	++
Cd39-null	+	++	−
Basal lamina			
Perlecan			
Wild type	++	+	++*
Cd39-null	++	++	++†
Fibrin			
Wild type	−	++	++
Cd39-null	−	++	+
Inflammatory cells			
F4/80			
Wild type	+	++	++
Cd39-null	+	+	+
Platelets			
Wild type	+	++	++
Cd39-null	+	++	−
B cells			
Wild type	+	−	−
Cd39-null	+	−	−
T cells			
Wild type	+	−	−
Cd39-null	+	−	−
Granulocytes			
Wild type	+	−	−
Cd39-null	+	−	−

−, <5 positively stained structures/hpf; +, 5 to 15 positively stained structures/hpf; ++, >15 positively stained structures/hpf.
*Associated with vasculature and muscle bundles.
†Associated with tumor nests.
NA, not applicable.

Endothelial Cell Proliferation in Vitro *Does Not Correlate with Defective Angiogenesis in Cd39-Null Mice* in Vivo

Purinergic signals have been implicated in promoting endothelial cell proliferation, as well as migration, during angiogenesis. However, we found no difference in endothelial proliferation by [^{3}H]thymidine uptake in wild-type and *Cd39*-null cells at baseline (100 ± 39% wild-type versus 97 ± 44% *Cd39*-null, $P = 0.47$) and after stimulation with VEGF (10 ng/ml) (135 ± 19% wild-type versus

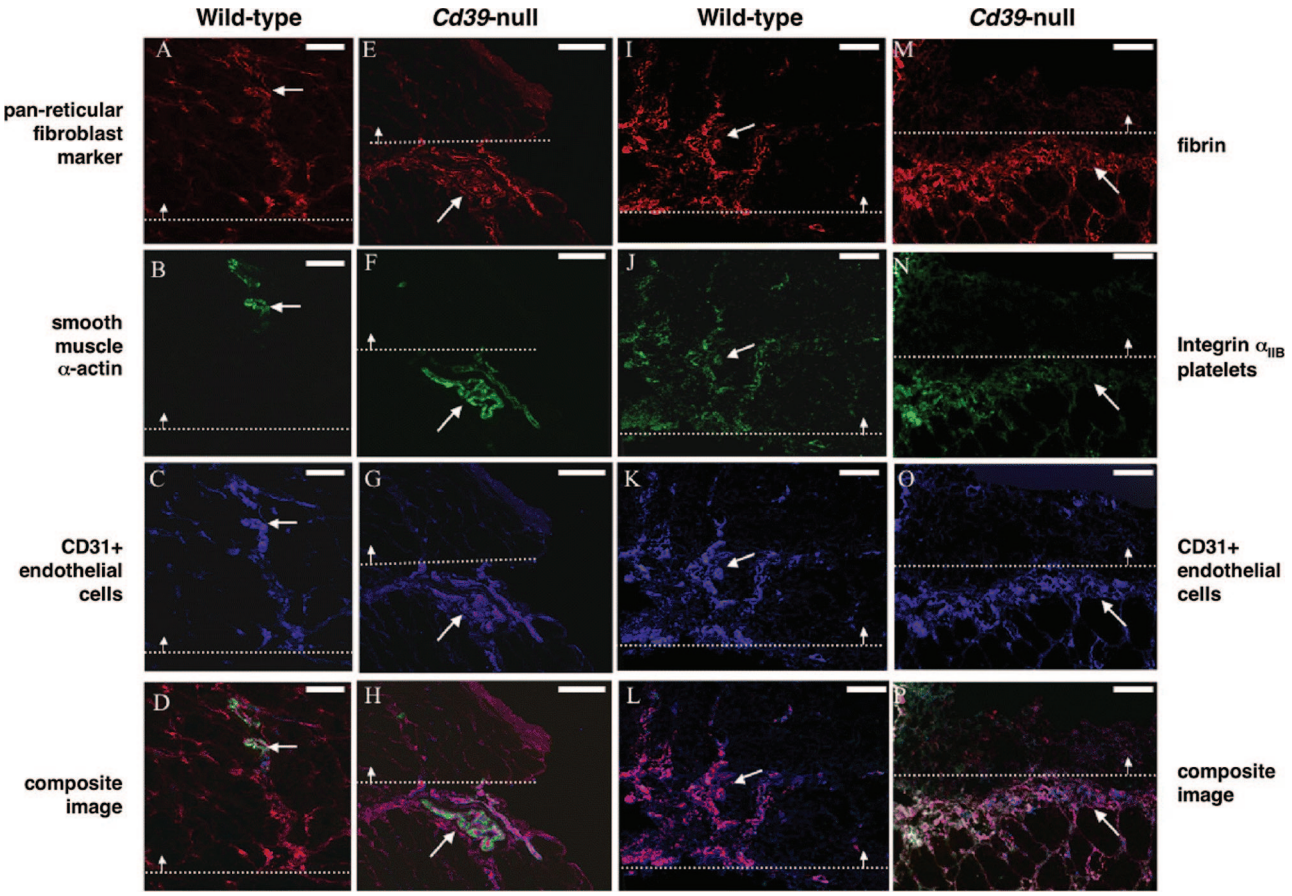

Figure 4. Triple immunofluorescent staining patterns of B16-F10 tumors. B16-F10 tumors were grown in the subcutaneous space in wild-type (**A–D**, **I–L**) and *Cd39*-null (**E–H**, **M–P**) mice and stained with antibodies recognizing: pericytes and fibroblasts (pan-reticular fibroblast marker) (**A** and **E**); pericytes and smooth muscle cells (smooth muscle α-actin) (**B** and **F**); fibrin (**I** and **M**); platelets (integrin α_{IIb}) (**J** and **N**); and endothelial cells (CD31) (**C**, **G**, **K**, and **O**) and their composites (**D**, **H**, **L**, and **P**). The **dotted white line** delineates the interface between the tumor mass and adjacent normal tissue. The **arrow** indicates the direction of the tumor. **A–D:** In tumors grown in wild-type mice the endothelial lining (blue) of vessels were only partially covered by mature smooth muscle α-actin-expressing pericytes (green) and interspersed in a network of interstitial fibroblasts (red). Note that the interstitial fibroblasts do not express smooth muscle α-actin. **E–H:** In *Cd39*-null mice, the endothelial lining (blue) of vessels in normal tissue adjacent to the tumor were to a large extent covered by smooth muscle α-actin-expressing pericytes (green) and surrounded by interstitial fibroblasts (red). Similar structures were absent within the actual tumor mass. **I–L:** In tumors in wild-type mice, a provisional matrix consisting of fibrin (red) and platelets (green) were associated with a large portion of CD31-positive (blue) tumor vessels (**arrow**). **M–P:** In *Cd39*-null mice fibrin (red) and platelets (green) were concentrated to a compacted rim of CD31 (blue)-positive vessels (**arrow**) at the interface between the tumor and normal adjacent tissue. Note nonspecific fluorescent staining in the central necrotic zone. Scale bars = 20 μm.

133 ± 37% *Cd39*-null, $P = 0.47$) *in vitro* (not shown). Similarly, we showed no difference in wild-type and *Cd39*-null endothelial cell proliferation after stimulation with a number of endothelial mitogens, including insulin, insulin-like growth factor-1, hepatocyte growth factor, and fibroblast growth factor (data also not shown). In addition, VEGF-induced activation of ERK1/2 was not attenuated in *Cd39*-null endothelial cells (Figure 5a).

Deletion of Cd39 Is Associated with Endothelial Cell-Selective Integrin Dysfunction

Purinergic signaling has been suggested to modulate the function of a number of integrins, including $\alpha_V\beta_3$, the vitronectin receptor.[10] Therefore, we measured the adhesion of wild-type and *Cd39*-null endothelial cells to a number of basement membrane substrates, including vitronectin. When contrasted to wild-type cells, *Cd39*-null endothelial cells exhibited normal, or near-normal, attachment to gelatin and fibronectin but had markedly decreased adhesion to vitronectin (Figure 5b). This defect was corrected by pretreatment of endothelial cells with soluble NTPDases (Figure 5c).

UTP has previously been shown to up-regulate the expression of the α_V integrin subunit in human umbilical vein endothelial cells.[18] However, we found no substantial difference between total α_V integrin levels in wild-type and *Cd39*-null endothelial cells. Nor did UTP increase the levels of α_V expression in either cell type by Western blot analysis (not shown). In addition, the surface expression of α_V was determined to be equal in wild-type and *Cd39*-null endothelial cells by immunofluorescence (data not shown). These data imply that qualitative differences in integrin activation are responsible, at least in part, for the defective adhesion phenotype.

$MnCl_2$ is a potent effector of a number of integrin-mediated adhesion events and is thought to activate integrins by binding to specific cation-binding sites and inducing conformational changes in the ligand-binding site.[19] In keeping with the hypothesis that $\alpha_V\beta_3$ activation is perturbed in

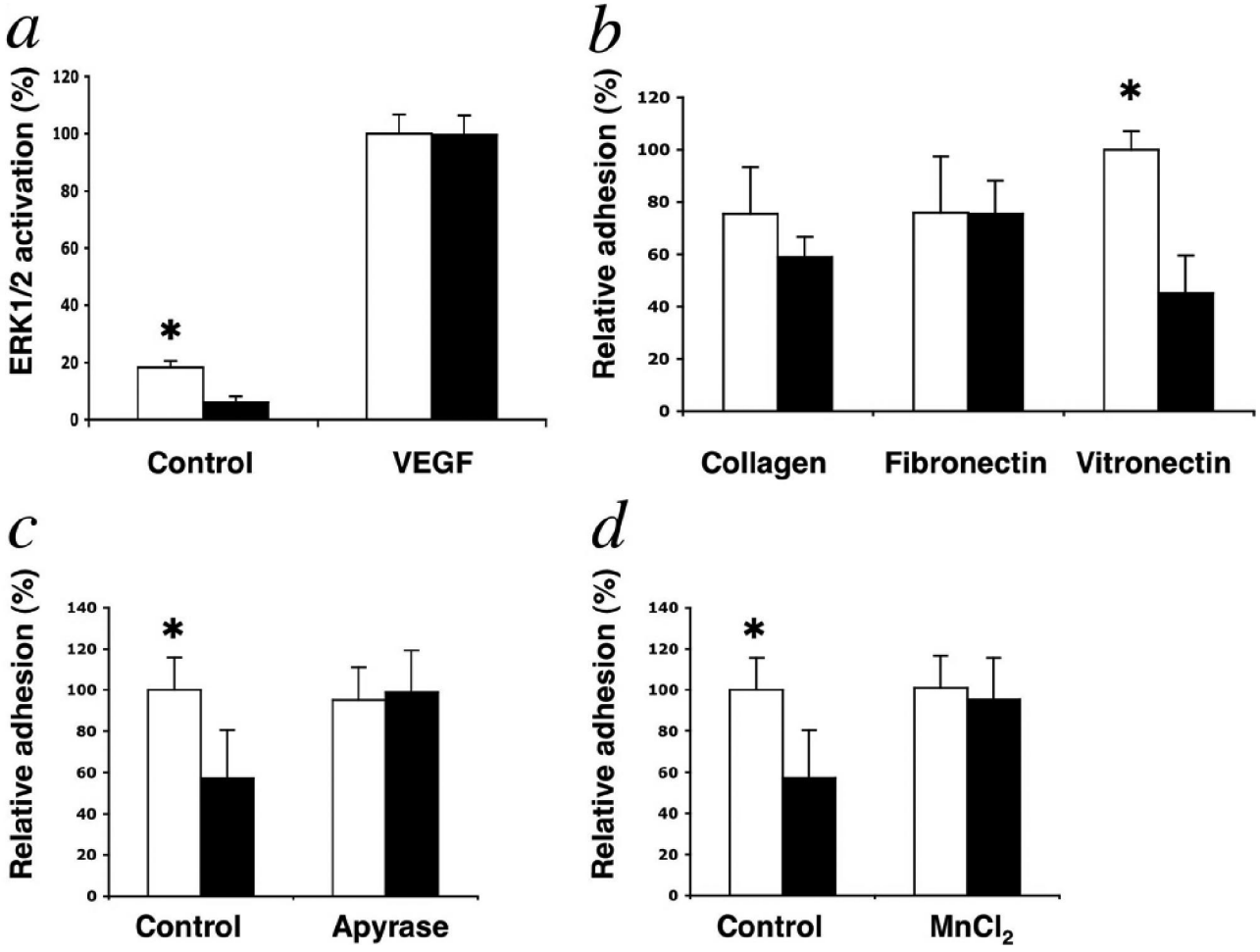

Figure 5. Cd39 deletion and associated integrin $\alpha_v\beta_3$ dysfunction. **a:** Phosphorylation of ERK1/2 (Thr202/Tyr204) in wild-type (□) and *Cd39*-null (■) endothelial cells at baseline and after stimulation with VEGF (10 ng/ml) for 5 minutes. Bar chart represents densitometry results (means ± SD) of phosphorylated ERK1/2 corrected for total ERK1/2. $^*P < 0.05$. **b:** Wild-type (□) and *Cd39*-null (■) endothelial adhesion to collagen, fibronectin, and vitronectin. Results expressed as a percentage of wild-type adhesion to collagen ± SEM. $^*P < 0.05$. **c:** Wild-type (□) and *Cd39*-null (■) endothelial cell adhesion to vitronectin after a 6-hour pretreatment with soluble apyrase (5 U/ml). Results expressed as mean percentage of wild-type adhesion to vitronectin ± SEM. $^*P < 0.05$. **d:** The α_v-integrin subunit expression in wild-type and *Cd39*-null endothelial cells was determined by immunoprecipitation and Western blot analysis. Cells were treated with UTP (100 μmol/L) for 0, 2, 4, and 6 hours. No differences were evident (not shown). Bar chart represents wild-type (□) and *Cd39*-null (■) endothelial cell adhesion to vitronectin after treatment with $MnCl_2$ (500 μmol/L). Results expressed as a percentage of wild-type adhesion to vitronectin ± SEM. $^*P < 0.05$.

Cd39-null endothelial cells, treatment with exogenous $MnCl_2$ was able to correct the defective adhesion of *Cd39*-null endothelial cells to vitronectin *in vitro* (Figure 5d).

Integrin-Associated Signaling Pathways in Cd39-Null Endothelial Cells

We also studied the effect of *Cd39* deletion on the downstream signaling pathways post-integrin ligation. In keeping with the defective adhesion of *Cd39*-null endothelial cells to vitronectin, deletion of *Cd39* was also associated with poor activation of FAK after $\alpha_V\beta_3$ ligation. Wild-type endothelial cells exhibited robust phosphorylation of FAK 15 and 30 minutes after plating onto vitronectin, whereas *Cd39*-null cells had significantly attenuated FAK activation (Figure 6a). FAK phosphorylation in *Cd39*-null cells was ~60% of the wild-type levels at 15 minutes ($P < 0.05$) and approximated half of wild-type levels at 30 minutes ($P < 0.05$). FAK activation reached wild-type levels in *Cd39*-null cells after 1 hour of adhesion (data not shown). In addition, the downstream activation of MAPK after integrin ligation was defective in *Cd39*-null cells. Phosphorylation of downstream ERK1/2 was half that of wild-type levels in *Cd39*-null endothelial cells at 30 minutes after vitronectin plating (Figure 6c, $P < 0.015$).

Decreased Activation of $\alpha_V\beta_3$ in Cd39-Null Endothelial Cells Is Associated with P2 Receptor Dysfunction

UTP has been shown to be chemoattractant to endothelial cells *in vitro*, implying a role for purinergic signaling in integrin activation.[4,18] We hypothesized that, analogous to platelets, *Cd39*-null endothelial cells undergo P2 receptor desensitization and associated integrin inactivation. To test this, we pretreated wild-type and *Cd39*-null endothelial cells with soluble NTPDases, to reconstitute

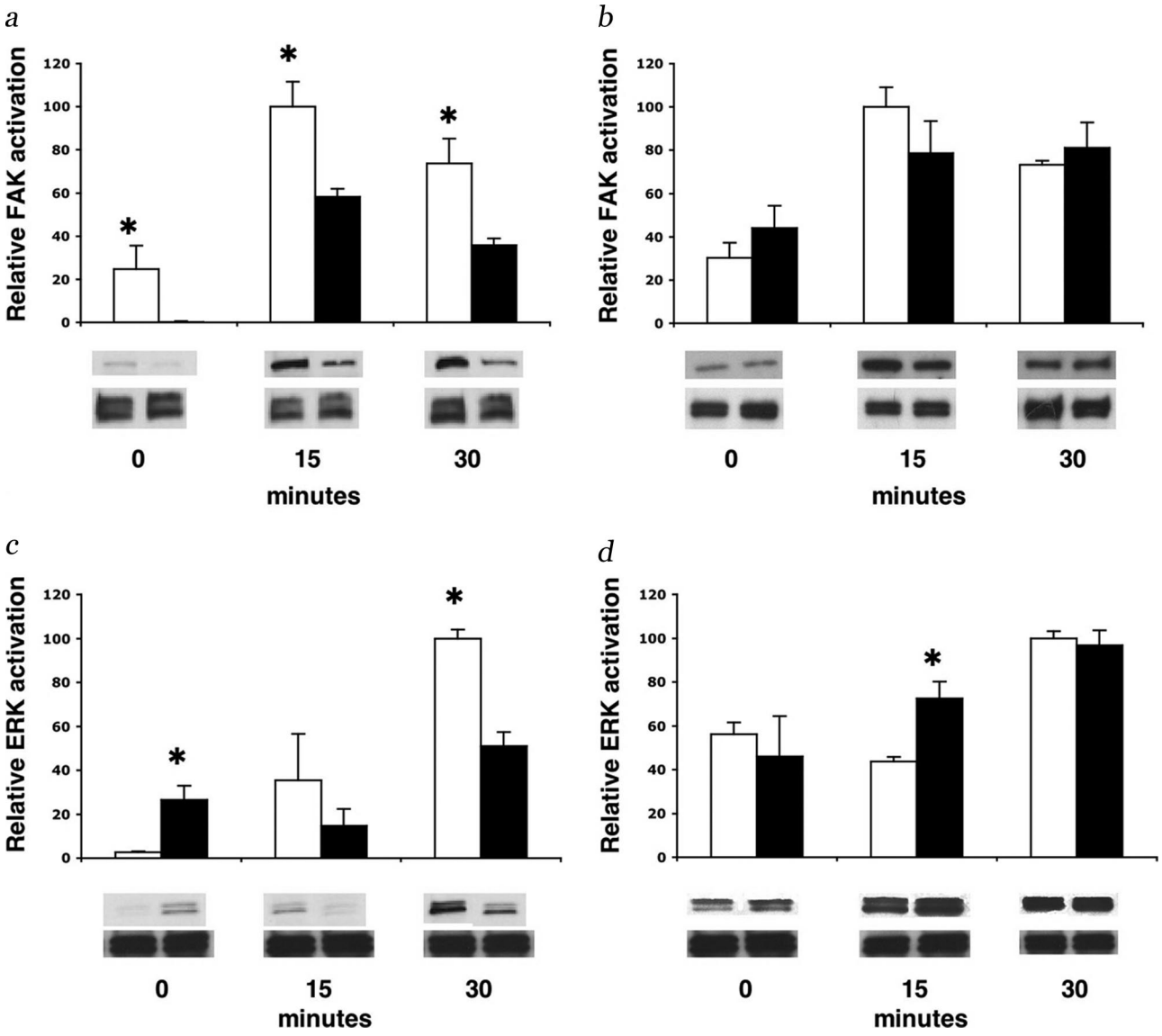

Figure 6. Deletion of Cd39 is associated with defective $\alpha_v\beta_3$-mediated intracellular signaling. **a** and **c:** Graphs represent phosphorylation of FAK (Tyr 397) (**a**) and ERK1/2 (Thr202/Tyr204) (**c**) in wild-type (□) and *Cd39*-null (■) endothelial cells at 0, 15, and 30 minutes after plating onto vitronectin. **b** and **d:** Phosphorylation of FAK (**b**) and ERK1/2 (**d**) in wild-type (□) and *Cd39*-null (■) endothelial cells pretreated for 6 hours with soluble Apyrase (5 U/ml). Bar charts represent densitometry results (means ± SEM) of phosphorylated FAK or ERK1/2 divided by total FAK or ERK1/2, respectively. $^*P < 0.05$. Representative blots are shown below graphs.

ecto-enzymatic functions of CD39 and restore P2 receptor functions, and then washed cells to remove residual apyrase activity before the adhesion assays.[3]

Apyrase pretreatment corrected the defective vitronectin adhesion of *Cd39*-null cells, as shown above (Figure 5c), and normalized the recruitment of FAK and downstream signaling to ERK1/2 to wild-type levels (Figure 6, b and d). Apyrase pretreatment had minimal effects on adhesion and on FAK and ERK1/2 activation in wild-type endothelial cells.

Discussion

We have shown that abnormal purinergic signaling in the *Cd39*-null vasculature results in profound defects in tumor growth and angiogenesis, indicating novel mechanisms of tumor angiogenesis. These data are consistent with our previous finding of defective angiogenesis studying Matrigel plug models in these mutant mice.[5]

Cd39-null mice exhibit the normal initial phases of angiogenesis, including mother vessel formation, increased vascular permeability, and fibrin deposition. However, there is a profound defect in the migration of endothelial and inflammatory cells into tumors in *Cd39*-null animals. Our *in vitro* data suggests that this defect is not caused by defects in endothelial proliferation. Although there are substantial defects in *Cd39*-null cellular adhesion noted *in vitro*, sequestration of injected tumor cells by the pulmonary vascular bed of *Cd39*-null mice does not contribute in a major way to the failure of metastatic tumor growth in these mutant mice. Importantly, there is markedly abnormal angiogenesis in *Cd39*-null mice charac-

terized by poor recruitment of surrounding pericytes and smooth muscle cells to new blood vessels. Because embryonic vascular development is normal in *Cd39*-null mice,[3] our data suggest that purinergic signaling has differential roles in physiological blood vessel development as opposed to pathological angiogenesis.

In vitro analyses indicate that the cellular migration defect in *Cd39*-null mice is likely to be secondary to abnormal adhesion and vitronectin receptor function in *Cd39*-null endothelial cells. The reconstitution of *Cd39*-null integrin function by apyrase pretreatment and the hydrolysis of extracellular nucleotides or by directed integrin effects by $MnCl_2$ implies that P2 receptor desensitization (and secondary integrin inactivation) is responsible for these findings (Figure 5).

Although several members of the integrin family have been implicated in angiogenesis, the largest body of data has linked the vitronectin receptor $\alpha_V\beta_3$ with the promotion of neovascularization. Numerous $\alpha_V\beta_3$ antagonists, including blocking antibodies directed at the extracellular domain of $\alpha_v\beta_3$ (LM609), inhibit angiogenesis in experimental animal models[9] and are currently undergoing human clinical trials.[20]

Despite the efficacy of these $\alpha_V\beta_3$ inhibitors, genetic deletion of $\alpha_V\beta_3$ paradoxically results in increased tumor angiogenesis.[21] It has been proposed that integrins might provide positive and/or negative signals to cells in the presence of appropriate extracellular ligands. The absence of these interactions could result in loss of putative negative signal(s) and enhanced angiogenesis.[22] These observations imply that $\alpha_V\beta_3$ could be involved in the fine-tuning of angiogenesis responses *in vivo*.

We have focused on elements of nucleotide-mediated signaling and shown that normal P2-type purinergic responses are required for $\alpha_V\beta_3$ function and for the process of angiogenesis. Cellular signaling by G protein-coupled receptors (GPCRs), such as P2Y receptors, involves not only the coupling of the receptors to G proteins but also the formation of large protein complexes that assist in transmitting an extracellular signal to an intracellular response.[23,24] $P2Y_2$ contains an integrin-binding, arginine-glycine-aspartic acid (RGD) domain in its first extracellular loop, suggesting interactions with integrin $\alpha_V\beta_3$. Mutation of the RGD sequence to RGE decreased the co-localization of α_v-integrins with $P2Y_2$ 10-fold and greatly impaired UTP-induced phosphorylation of FAK.[10]

Direct association between $P2Y_2$ and α_v-integrins seems to also be necessary for UTP-induced endothelial cell migration, implying an important link between purinergic signaling, integrin function, and proangiogenic cellular behaviors.[18] It has previously been shown that ATP and UTP activate FAK by calcium-dependent signaling mechanisms.[18] The $\alpha_V\beta_3$integrin-mediated activation of FAK can be shown to be defective in *Cd39*-null endothelial cells. Deletion of *Cd39* results in differential P2 receptor desensitization, which subsequently modulates the activity of $\alpha_V\beta_3$. In keeping with this supposition, apyrase pretreatment of *Cd39*-null endothelial cells, which corrects P2 receptor desensitization, normalizes $\alpha_V\beta_3$ functions.

We have recently noted that the N terminus of CD39 interacts with the multiadaptor scaffolding membrane phosphoprotein RanBPM.[25] RanBPM binds the hepatocyte growth factor receptor cMET and modulates the Ras-ERK-SRE pathway.[26] In addition, RanBPM interacts with integrins such as LFA-1 (lymphocyte function-associated antigen-1) and may affect signaling pathways directly.[27] These results suggest that CD39 may regulate cellular signal transduction pathways and integrin function by two separate mechanisms: by first modulating P2 receptor function after hydrolysis of extracellular nucleotides, and secondly, by interacting with other signaling proteins directly, possibly using RanBPM as a bridge.

There are other potential factors that could be also impacted on by the NTPDase1 biochemical functions. In addition to modulating P2 receptor signaling by nucleotide hydrolysis and scavenging, CD39 in association with CD73 ultimately generates adenosine, which also has important proangiogenic functions. For example, adenosine, acting via the A_{2A} receptor, promotes wound healing by stimulating angiogenesis.[28] Second, the A_{2A} receptor has recently been implicated in the inhibition of antitumor T cells within the adenosine-rich tumor microenvironment.[29]

In these currently submitted angiogenesis studies, we have preferentially detailed the role of endothelial cell integrin dysfunction in *Cd39*-null mice. Some aspects of the *Cd39*-null antitumor phenotype could further be explained by decreased adenosine generation. In this regard, we have evidence that CD39 forms an important part of the immunosuppressive apparatus of regulatory T cells (Treg), at least in part via the generation of adenosine.[30] We do not address the role of T cells in immune regulation of tumors here.

In conclusion, we have provided evidence for the importance of extracellular nucleotides in modulating endothelial cell responses in models of pathological angiogenesis. We have also described novel links between purinergic signaling and integrin activation that are modulated by CD39. These findings raise the possibility of new anti-angiogenesis therapies based on modulating extracellular nucleotide-mediated signals. These goals could be achieved by either blocking the action of CD39 directly or by targeting those nucleotide (P2) receptors that are crucial in the process of angiogenesis.

Acknowledgments

We thank Dr. Julie Lively, Medicine, Beth Israel Deaconess Medical Center, for help with endothelial cellular cultures; and Dr. Takashi Murakami, Jichi Medical Center, for the kind gift of luciferase-expressing B16/F10 cells (lucB16/F10).

References

1. Kaczmarek E, Koziak K, Sevigny J, Siegel JB, Anrather J, Beaudoin AR, Bach FH, Robson SC: Identification and characterization of CD39/vascular ATP diphosphohydrolase. J Biol Chem 1996, 271: 33116–33122
2. Fredholm BB, Abbracchio MP, Burnstock G, Daly JW, Harden TK,

Jacobson KA, Leff P, Williams M: Nomenclature and classification of purinoreceptors. Pharmacol Rev 1994, 46:143–152
3. Enjyoji K, Sevigny J, Lin Y, Frenette PS, Christie PD, Esch JS, Imai M, Edelberg JM, Rayburn H, Lech M, Beeler DL, Csizmadia E, Wagner DD, Robson SC, Rosenberg RD: Targeted disruption of Cd39/ATP diphosphohydrolase results in disordered hemostasis and thromboregulation. Nat Med 1999, 5:1010–1017
4. Satterwhite CM, Farrelly AM, Bradley ME: Chemotactic, mitogenic, and angiogenic actions of UTP on vascular endothelial cells. Am J Physiol 1999, 45:H1091–H1097
5. Goepfert C, Sundberg C, Sevigny J, Enjyoji K, Hoshi T, Csizmadia E, Robson SC: Disordered cellular migration and angiogenesis in Cd39-null mice. Circulation 2001, 104:3109–3115
6. Hanahan D, Folkman J: Patterns and emerging mechanisms of the angiogenic switch during tumorigenesis. Cell 1996, 86:353–364
7. Carmeliet P, Jain RK: Angiogenesis in cancer and other diseases. Nature 2000, 407:249–257
8. Carmeliet P: Mechanisms of angiogenesis and arteriogenesis. Nat Med 2000, 6:389–395
9. Hodivala-Dilke KM, Reynolds AR, Reynolds LE: Integrins in angiogenesis: multitalented molecules in a balancing act. Cell Tissue Res 2003, 314:131–144
10. Erb L, Liu J, Ockerhausen J, Kong Q, Garrad RC, Griffin K, Neal C, Krugh B, Santiago-Perez LI, Gonzalez FA, Gresham HD, Turner JT, Weisman GA: An RGD sequence in the P_2Y_2 receptor interacts with $\alpha_V\beta_3$ integrins and is required for G_o-mediated signal transduction. J Cell Biol 2001, 153:491–501
11. Parsons JT: Focal adhesion kinase: the first ten years. J Cell Sci 2003, 116:1409–1416
12. Berra E, Milanini J, Richard DE, Le Gall M, Vinals F, Gothie E, Roux D, Pages G, Pouyssegur J: Signaling angiogenesis via p42/p44 MAP kinase and hypoxia. Biochem Pharmacol 2000, 60:1171–1178
13. Shih IM, Torrance C, Sokoll LJ, Chan DW, Kinzler KW, Vogelstein B: Assessing tumors in living animals through measurement of urinary β-human chorionic gonadotropin. Nat Med 2000, 6:711–714
14. Sato A, Ohtsuki M, Hata M, Kobayashi E, Murakami T: Antitumor activity of IFN-λ in murine tumor models. J Immunol 2006, 176:7686–7694
15. Maeshima Y, Colorado PC, Torre A, Holthaus KA, Grunkemeyer JA, Ericksen MB, Hopfer H, Xiao Y, Stillman IE, Kalluri R: Distinct antitumor properties of a type IV collagen domain derived from basement membrane. J Biol Chem 2000, 275:21340–21348
16. Hodivala-Dilke KM, McHugh KP, Tsakiris DA, Rayburn H, Crowley D, Ullman-Cullere M, Ross FP, Coller BS, Teitelbaum S, Hynes RO: β_3-Integrin-deficient mice are a model for Glanzmann thrombasthenia showing placental defects and reduced survival. J Clin Invest 1999, 103:229–238
17. Palumbo JS, Kombrinck KW, Drew AF, Grimes TS, Kiser JH, Degen JL, Bugge TH: Fibrinogen is an important determinant of the metastatic potential of circulating tumor cells. Blood 2000, 96:3302–3309
18. Kaczmarek E, Erb L, Koziak K, Jarzyna R, Wink MR, Guckelberger O, Blusztajn JK, Trinkaus-Randall V, Weisman GA, Robson SC: Modulation of endothelial cell migration by extracellular nucleotides: involvement of focal adhesion kinase and phosphatidylinositol 3-kinase-mediated pathways. Thromb Haemost 2005, 93:735–742
19. Smith JW, Piotrowicz RS, Mathis D: A mechanism for divalent cation regulation of β_3-integrins. J Biol Chem 1994, 269:960–967
20. Gutheil JC, Campbell TN, Pierce PR, Watkins JD, Huse WD, Bodkin DJ, Cheresh DA: Targeted antiangiogenic therapy for cancer using Vitaxin: a humanized monoclonal antibody to the integrin $\alpha_V\beta_3$. Clin Cancer Res 2000, 6:3056–3061
21. Reynolds LE, Wyder L, Lively JC, Taverna D, Robinson SD, Huang X, Sheppard D, Hynes RO, Hodivala-Dilke KM: Enhanced pathological angiogenesis in mice lacking β_3 integrin or β_3 and β_5 integrins. Nat Med 2002, 8:27–34
22. Carmeliet P: Integrin indecision. Nat Med 2002, 8:14–16
23. Pierce KL, Premont RT, Lefkowitz RJ: Signalling: seven-transmembrane receptors. Nat Rev Mol Cell Biol 2002, 3:639–650
24. Hall RA, Lefkowitz RJ: Regulation of G protein-coupled receptor signaling by scaffold proteins. Circ Res 2002, 91:672–680
25. Wu Y, Sun X, Kaczmarek E, Dwyer KM, Bianchi E, Usheva A, Robson SC: RanBPM associates with CD39 and modulates ecto-nucleotidase activity. Biochem J 2006, 396:23–30
26. Wang D, Li Z, Messing EM, Wu G: Activation of Ras/Erk pathway by a novel MET-interacting protein RanBPM. J Biol Chem 2002, 277:36216–36222
27. Denti S, Sirri A, Cheli A, Rogge L, Innamorati G, Putignano S, Fabbri M, Pardi R, Bianchi E: RanBPM is a phosphoprotein that associates with the plasma membrane and interacts with the integrin LFA-1. J Biol Chem 2004, 279:13027–13034
28. Montesinos MC, Shaw JP, Yee H, Shamamian P, Cronstein BN: Adenosine A_{2A} receptor activation promotes wound neovascularization by stimulating angiogenesis and vasculogenesis. Am J Pathol 2004, 164:1887–1892
29. Ohta A, Gorelik E, Prasad SJ, Ronchese F, Lukashev D, Wong MKK, Huang X, Caldwell S, Liu K, Smith P, Chen J, Jackson EK, Apasov S, Abrams S, Sitkovsky M: A_{2A} adenosine receptor protects tumors from antitumor T cells. Proc Natl Acad Sci USA 2006, 103:13132–13137
30. Deaglio S, Dwyer KM, Gao W, Friedman D, Usheva A, Erat A, Chen JF, Enjyoji K, Linden J, Oukka M, Kuchroo VK, Strom TB, Robson SC: Adenosine generation catalyzed by CD39 and CD73 expressed on regulatory T cells mediates immune suppression. J Exp Med 2007, 204:1257–1265